

# SEGMENTATION OF MAMMOSPHERE STRUCTURES FROM VOLUMETRIC DATA

Ju Han, Hang Chang, Qing Yang, Mary Helen Barcellos-Hoff and Bahram Parvin

Lawrence Berkeley National Laboratory, Berkeley, CA 94720

## ABSTRACT

3D cell culture assays have emerged as the basis of an improved model system for evaluating therapeutic agents, molecular probes, and exogenous stimuli. However, there is a gap in robust computational techniques for segmentation of image data that are collected through confocal or deconvolution microscopy. The main issue is the volume of data, overlapping subcellular compartments, and variation in scale and size of subcompartments of interest. A *geometric* technique has been developed to bound the solution of the problem by first localizing centers of mass for each cell and then partitioning clumps of cells along minimal intersecting surfaces. An approximate solution to the center of mass is realized through iterative spatial voting, which is tolerant to variation in shape morphologies and overlapping compartments and is shown to have an excellent noise immunity. These approximate estimates to centers of mass are then used to partition a clump of cells along minimal intersecting surfaces that are estimated by Radon transform. Examples on real data and performance of the system over a large population of data are evaluated. Furthermore, it is shown that the proposed methodology is extensible in terms of its application to protein localization studies.

## 1. INTRODUCTION

Current models of high-throughput and high-content screening are based on two-dimensional cell culture assays that are grown either on plastic or glass. Although such a model system may be appropriate as an initial step toward discovery or for certain aspects of biological studies, the knowledge may not be readily extensible to *in vivo* models. On the other hand, animal studies are expensive and time-consuming and as a result cannot scale for high-throughput studies that are necessary to build a space-time continuum of responses in the presence of biological heterogeneity. An intermediate step is three-dimensional cell culture model systems, which have been demonstrated to have some of the functionalities of the *in vivo* models. However, such a model system introduces significant computational challenges: (i) imaging is in 3D and not in projection space, (ii) subcellular compartments often overlap and delineation is made difficult, and (iii) variations in subcellular scale imposes a more complex segmentation problem at the object level. In this paper, we present a series of geometric steps for segmentation of 3D cell culture models, also known as acini, that enables subsequent localization studies and protein-protein interactions.

Research in the analysis of subcellular structures spans texture-based features for classifying patterns of protein expression [6], geometric methods [9], and surface evolution methods [4] for delineation of nuclear compartments. Segmentation of a subcellular compartment provides context for quantifying protein localization in fixed samples with an antibody or a nucleic-acid-based probe in living cell

studies. However, most of the previous techniques are not applicable for automated segmentation of mammospheres labeled by their nuclear compartments, and the proposed solution bounds an inherently ill-posed problem through geometric constraints. A key observation is that nuclear regions are often convex and form a positive curvature maxima when they overlap each other. This feature was used earlier in 2D segmentation of nuclear regions [9]. However, evaluating 3D convexity and estimating 3D surface curvature is hindered by significant computational complexities.

In image understanding, saliency or perceptual grouping [3, 5] can be driven by continuity [11], symmetry, or closure. Among these, it is well known that symmetry is a pre-attentive process [1] that improves recognition, provides an efficient mechanism for scene representation, and aids in reconstruction and description. Radial symmetry is a special class of symmetry, which persists in nature at multiple scales. Robust and efficient detection of inexact radial symmetries facilitates the semantic representation of images for summarization and interpretation. Yet, the notion of radial symmetry is used in a weak sense since the basic geometry can deviate in aspect ratio and convexity. At the coarse scale, localization of the approximate centroid of each nucleus in a three dimensional cell culture assay enables partitioning a mammosphere along the planes that generate minimum surface cross sections and are possibly aligned with points of maximum curvature along the surface. At the fine scale, localization of punctate and radial protein events within each nucleus enables an accurate representation of cause and effect.

The novelty of the proposed method is in specific geometric steps designed to bound the solution through seeding and subsequent partitioning. The basis for seeding is through geometric voting and perceptual grouping, and is implemented through the refinement of specifically tuned voting kernels [8]. The method has excellent noise immunity, is tolerant of variations in target shape scale, and is applicable to a large class of application domains. Localization of centers of mass for each nucleus provides a bound on overall stable segmentation. Nuclei are connected each other in a mammosphere where the adaptive thresholding cannot provide enough nuclear partition information. Therefore, the nuclei are initially segmented by Voronoi tessellation of the nuclear seeds and the results are refined by the Radon transform. Nuclear segmentation provides the context localization studies under different experimental treatments. In some cases, protein localization may be punctate (e.g., DNA repair protein). These punctate signals can be further segmented to quantify a specific biophysical properties. Segmentation of these sparse and noisy punctate signals can also be realized through seed estimation at a finer scale followed by modeling the intensity distribution as a mixture of Gaussian for subsequent local thresholding.

## 2. PREVIOUS RESEARCH

Current state of art for delineating nuclear regions from multicellular systems has been limited to intensity-based information, and geometric information are largely under-utilized. Some of these methods are interactive and serve as a computer-aided tool to increase

---

THIS WORK IS SUPPORTED IN PART BY THE DIRECTOR, OFFICE OF ENERGY SCIENCE RESEARCH, OFFICE OF MEDICAL SCIENCES, LIFE SCIENCES OF THE U. S. DEPARTMENT OF ENERGY AND NASA UNDER CONTRACT NO. DE-AC03-76SF00098 WITH THE UNIVERSITY OF CALIFORNIA. LBNL-PUBID IS 62476.

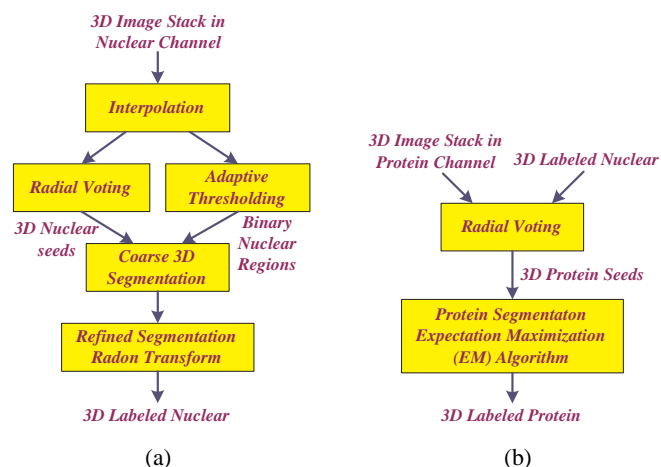


**Fig. 1.** Computational steps in segmentation and localization: (a) segmentation of nuclear channels provides context for localization studies; and (b) segmentation of punctate protein events provides quantitative data for characterizing biophysical properties.

operational throughput. In [7], background and nuclear regions are delineated with automatic thresholding. The nuclear size is then estimated with the Hough transform, which provides an initial constraint for a watershed-based delineation. In [10], limitations in [7] were identified: (1) initial thresholding, (2) noise, and (3) low gradient in some of the nuclear regions. These limitations were then addressed using level set methods for improved performance. In [12], nuclear regions were modeled as elliptic features and fragmented features were grouped together to form a convex hull. The method produces a segmentation that is not very accurate along the surfaces with potential fragmentation of nuclear regions. Recently, in [2], mammosphere slices were segmented in 2D and then segmented 2D slices were merged together. However, the assay produced nuclear regions that tend to be separable in 2D (e.g., little overlap) while maintaining similar scale in nuclear size. Heterogeneity in these assays originate from cell line (e.g., normal or tumorigenic) and specific treatments that they go under.

In contrast to previous approaches, the proposed method uses high level geometric features to delineate a multicellular system. Geometrically, nuclear regions are almost convex; however, scale (e.g., size) is heterogeneous. Furthermore, when two nuclear regions overlap, they form folds corresponding to positive curvature maxima. Partitioning adjacent nuclear regions along points of curvature maxima, or a variation of that, is the final step of the process.

### 3. APPROACH

Specific steps in delineation of nuclei and localization of proteins in a mammosphere system are shown in Figure 1. Both nuclear segmentation and protein localization are initialized by seed localization via radial voting. Voronoi tessellation followed by the Radon transform is used for nuclear segmentation due to the mass connectivity of nuclei; while the expectation maximization algorithm is performed to separate sparsely distributed proteins from the noisy background in a partitioned nucleus.

Starting from the interpolated 3D image in nuclear channel, the solution is initially bounded by computing seeds that provide an estimate to the location of the centroid of each nucleus through iterative radial voting. Simultaneously, the colony is thresholded in 3D, which produces an erroneous segmentation of the clump of nearby cells by merging them. Each clump is subsequently labeled for fur-

ther analysis, and any connected volume with more than two seeds is subject for further analysis. Partitioning is performed by finding planes that best separate adjacent nuclei, and the actual methodology is based on the Radon transform. However, Radon transfer precedes by a coarse segmentation from adjacent seed locations. Ideally, such a coarse segmentation should be realized through voronoi tessellation, which is compute intensive in 3D. A simpler approximation to voronoi tessellation is implemented to provide a rough segmentation of nuclear regions. This segmentation is further refined by Radon transform. Nuclear segmentation provides the context for protein localization, which may be heterogeneous in each mammosphere. In some cases, protein localization is punctate. These punctate signals can also be detected through 2D radial voting and accurately segmented in the secondary channel that visualizes proteins of interest. The intensity distribution of these punctate signals is modeled as a Gaussian mixture model, where the latent variables can be estimated with the expectation maximization algorithm.

#### 3.1. Nuclear seed estimation with iterative voting

The basis for seeding (e.g., estimating centers of mass) is through geometric voting and perceptual grouping, and is implemented through the refinement of specifically tuned voting kernels [8]. In general, voting operates on the notion of continuity and proximity, which can occur at multiple scales, e.g., points, lines, lines of symmetry, or generalized cylinders. The novelty of our approach is in defining a series of kernels that vote iteratively along the radial or tangential directions. Voting along the radial direction leads to localization of the center of mass, while voting along the tangential direction enforces continuity. At each iteration, the kernel orientation is refined until it converges to a single focal response. Voting kernels have a cone-shaped with an initial scale and spread (e.g., height and base) that is refined iteratively. These kernels are initially applied along the gradient direction, then at each consecutive iteration and at each grid location, orientation is aligned along the maximum local response. The method has excellent noise immunity, is tolerant to variations in target shape scale, and is applicable to a large class of application domains. Figure 2 shows a subset of voting kernels that vary in topography, scale, and orientation.

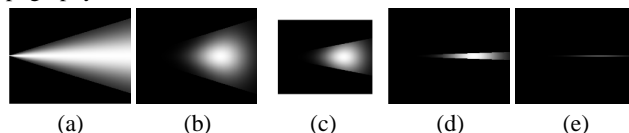


**Fig. 2.** Kernel topography: (a-e) Evolving kernel for the detection of radial symmetries (shown at a fixed orientation) has a trapezoidal active area with Gaussian distribution along both axes.

To illustrate the behavior of iterative voting, Figure 3 shows intermediate steps that leads toward final results for overlapping 2D objects that are generated synthetically. The voting landscape corresponds to the spatial clustering that is initially diffuse and is subsequently refined and focused into distinct regions. An example of the 3D voting is shown in Figure 4, where each nucleus in a mammosphere has been detected.

#### 3.2. Partitioning of a mammosphere from seeded nuclei

The process is initiated by a coarse segmentation of nuclei with a 3D voronoi tessellation. Tessellation facilitates (1) identification of a local neighborhood where each nuclear region is contained within its own space, and (2) improved computational performance. The first feature has to do with constrained locality, which eliminates error and reduces ambiguities. Without tessellation, Radon transfer will fail because two neighboring nuclei may have a third nucleus

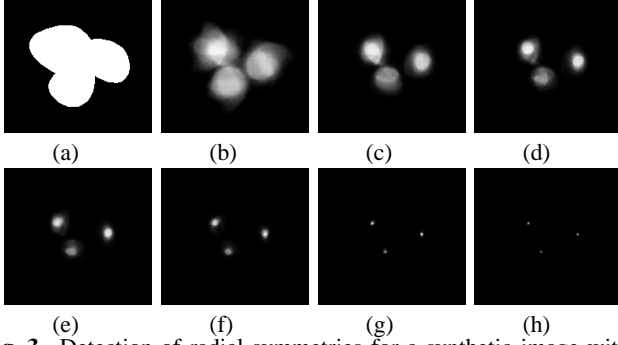


**Fig. 3.** Detection of radial symmetries for a synthetic image with multiple overlapping objects: (a) original image; (b)-(g) voting landscape at each iteration; and (h) final localization of centers of mass.

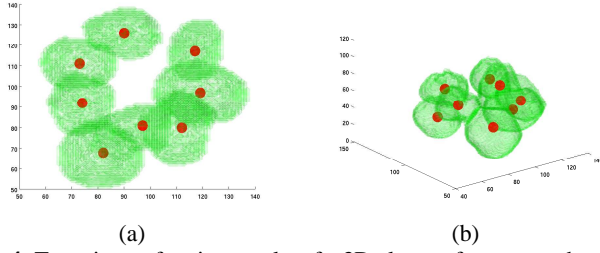


**Fig. 4.** Two views of voting results of a 3D clump of mammosphere: (a) top view; (b) side view.

that sits at the fold of the two touching nuclei. The second feature has to do with the fact that not all adjacent nuclei are connected and that there is a clear empty space between them. Under this condition, there is no need to refine the segmentation further.

The details of Radon transform are as follows; however, for simplicity the 2D version is first described. The Radon transform represents an image as a collection of projections in a function domain  $f(x, y)$  along various lines defined by the shortest distance  $\rho$  from the origin and the angle of inclination  $\theta$  with the  $y$  axis:

$$R(\rho, \theta) = \int f(x, y) \delta(\rho - x \cos \theta - y \sin \theta) dx dy. \quad (1)$$

Properties of the Radon transform enable delineation of nearby touching objects. For example, two adjacent objects, represented by circles in Figure 5(a), and their corresponding Radon transform shown in Figure 5(b), have a local minimum that is located at  $\rho = 17$  and  $\theta = 135^\circ$ . This local minimum corresponds to the integration over the line that separates the two objects with the smallest cross section.

Similarly, the 3D Radon transform represents a 3D volume as a collection of projections in a function domain  $f(x, y, z)$  along various planes defined by the shortest distance  $\rho$  from the origin, the angle of azimuth  $\phi$  around the  $z$  axis and the angle of elevation  $\theta$  around the  $y$  axis:

$$R = \int f(x, y, z) \delta(\rho - x \cos \phi \cos \theta - y \sin \phi \cos \theta - z \sin \theta) dx dy dz$$

The 3D Radon transform is separable and the 3D Radon transform can be decomposed into a series of 2D Radon transforms. Given a local cube containing two nearby adjacent cells, each of which is bounded by a seed, the optimal plane separating these two cells should be located between the two seeds and have the smallest cross section. The local minimum in the 3D Radon transform corresponds to the integration over the optimal plane in the local cube. Figure 6 shows an example of nuclear segmentation results.

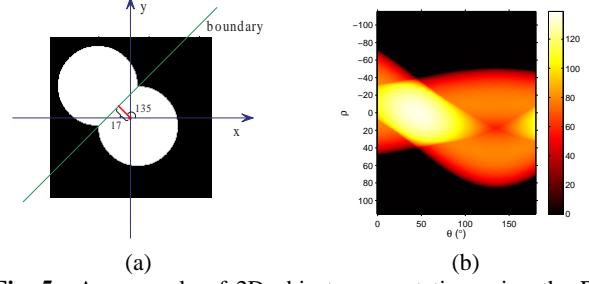


**Fig. 5.** An example of 2D object segmentation using the Radon transform: (a) synthetic object composed of two circles; and (b) corresponding Radon transform with local minimum at  $\rho = 17$  and  $\theta = 135^\circ$ .

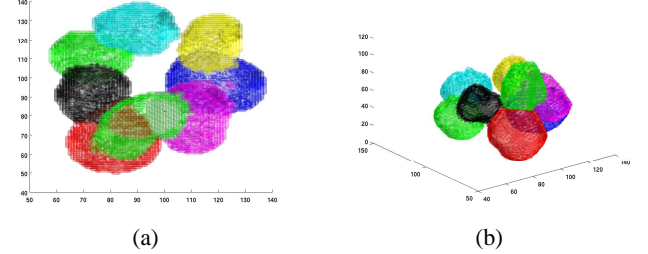


**Fig. 6.** Two views of final segmentation of a mammosphere: (a) top view; (b) side view.

### 3.3. Protein localization

Nuclear segmentation provides context for quantitative assessment of protein localization, which may not necessarily be diffused. For example, nuclear foci formation are punctate and are formed by phosphorylation of histone  $\gamma$ H2AX following ionizing radiation. These punctate features can also be detected with radial voting, at a much smaller scale, within each 3D connected component. Accurate segmentation of these punctate events can reveal certain properties that are of interest for biophysical modeling. This kind of functionality is often referred to as the interest point operator and there is a large literature on this topic, but iterative voting is robust and can distinguish overlapping events. However, segmentation of punctate events can be complex as a result of variations in (1) foci size, (2) background intensity, (3) foreground intensity, (4) sample preparation, and (5) potential cross-talk between neighboring foci. While voting provides an initial localization of foci, a robust method for accurate segmentation is needed. Our approach is based on (1) establishing a local neighborhood for each foci, which is also bounded by the maximum size of the foci, and (2) modeling the local intensity distribution as a mixture of two Gaussians, where the latent variables are estimated using the expectation-maximization method. The technique has been validated on synthetic data with and without noise, and then applied to real data.

Let the mixture Gaussian density model be expressed as:  $p(\mathbf{x}|\Theta) = \sum_{i=1}^M \alpha_i p_i(\mathbf{x}|\theta_i)$ , where  $\sum_{i=1}^M \alpha_i = 1$ , and each  $p_i$  is a Gaussian density function parameterized by  $\theta_i$ . That is, each  $\mathbf{x}$  may be generated from any of the  $M$  distributions with different probabilities, where  $M = 2$ . By considering  $\mathcal{X} = \{\mathbf{x}_i\}_{i=1}^N$  as *incomplete* data, and introducing *unobservable* data as  $\mathcal{Y} = \{y_i\}_{i=1}^N$  (where  $y_i \in 1, \dots, M$  and whose values indicate which component density generates each  $\mathbf{x}_i$ ), the log-likelihood function can be simplified as

$$\begin{aligned} \log(\mathcal{L}(\Theta|\mathcal{X}, \mathcal{Y})) &= \log(P(\mathcal{X}, \mathcal{Y}|\Theta)) \\ &= \sum_{i=1}^N \log(P(\mathbf{x}_i|y_i)P(y_i)) = \sum_{i=1}^N \log(\alpha_{y_i} p_{y_i}(\mathbf{x}_{y_i}|\theta_{y_i})) \end{aligned}$$

where the parameters  $\theta_i$  and the latent variable  $\mathcal{Y}$  can be estimated with the EM approach. The EM algorithm is a two-step iterative optimization technique that maximizes the expectation of the log-likelihood function, conditioned on the observed data and the current estimate of  $\Theta$ :

- *Expectation step*: At the  $n$ -th iteration, given the observed data  $\mathcal{X}$  and the current estimate  $\Theta^{n-1}$ , construct the expectation of the log-likelihood function with respect to the unknown random variable  $y$ :  $Q(\Theta, \Theta^{n-1}) = E [\log P((\mathcal{X}, \mathcal{Y})|\Theta, \Theta^{n-1})]$ .

- *Maximization step*: Compute the next estimation of  $\Theta$  by maximizing  $Q(\Theta, \Theta^{n-1})$ :  $\Theta^n : \frac{\partial Q(\Theta, \Theta^{n-1})}{\partial \Theta} = 0$ .

The EM algorithm initiates from an estimate  $\Theta^0$ , which is refined iteratively, and terminates when  $\|\Theta^n - \Theta^{n-1}\|$  is less than a small threshold. The  $\mathcal{Y}$  values so-obtained at the final iteration label each data sample in  $\mathcal{X}$ . Figure 7 shows an example of protein localization results in partitioned nuclei.

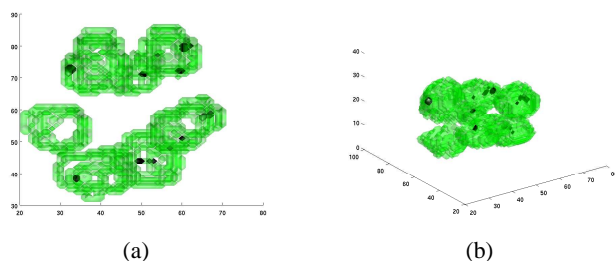


**Fig. 7.** Two views of localization of protein in partitioned nuclei: (a) top view; (b) side view.

#### 4. EXPERIMENTAL RESULTS

The proposed approach was implemented and applied in a data set of mammospheres, imaged with deconvolution microscopy. The image resolution along the  $x$  and  $y$  directions is  $0.15\mu m$ , and the resolution along the  $z$  direction is  $1.32\mu m$ . 151 colonies in the data set with an average of 11 seeds per colony were processed using the proposed approach and the same input parameters. 1771 seeds were estimated through iterative radial voting; however, 77 nuclei did not register any corresponding seeds, which indicates a detection error rate of 4%. This is presumably due to abnormal scale and shape of the nuclear volume, and the exact conditions are as follows:

- *Low contrast between overlapping nuclei*: Absence of gradient information between overlapping nuclei coupled with their accidental morphological properties provide ambiguous voting evidence that produces one fixed point instead of two.

- *Morphological abnormality*: Often a single nucleus has an abnormal elongated shape and radial voting merges multiple seed points into a single fixed point. This condition is highly correlated with the previous case.

- *Incomplete information*: This is an imaging problem, where imaging is incomplete and part of the nuclei is missing from the volumetric image.

- *Low sampling resolution in Z axis*: The current interpolation algorithm is linear for making a volumetric stack homogeneous in its X, Y, and Z dimension. Linear interpolation smoothes the gradient in the Z direction and reduces the contribution of the corresponding gradient information. An improved model will use some form of spline interpolation.

Finally, partitioning accuracy was compromised for 35 pairs of overlapping nuclei from a total of 1850 pairs, which indicates an error rate of approximately 2%. These errors occur when the optimum plane for separating two nuclei is not the desired plane for partitioning two neighboring nuclei. The notion of desired planes has to do

with those planes that bisect neighboring nuclei along points of maximum curvature. In this case, the error rate can be reduced through improved seed localization.

#### 5. CONCLUSION

This paper presented a series of geometric steps for segmentation of mammospheres in 3D. The first step localizes an approximation to center of mass for each nucleus and then partitions a clump of nuclei along minimal intersecting surfaces. Approximate solution to the center of mass is realized through iterative spatial voting, which is tolerant to variation in shape morphologies, perceptual surfaces, noise, and overlapping compartments. These centers of mass are then used to partition a clump of cells along minimal intersecting surfaces that are estimated by Radon transform. The technique has been tested on 151 colonies and their corresponding 3D volumes, and error rate is fully characterized. Segmentation of the mammosphere has provided the context for localization studies, where we have shown how components of the same method can be used to characterize punctate signals within the nuclear region.

*Acknowledgment*: Authors thank Dr. Sylvain Costes for generation of the dataset used in this study.

#### 6. REFERENCES

- [1] F. Attneave. Symmetry information and memory for patterns. *American Journal of Psychology*, 68:209–222, 1955.
- [2] D. Knowles, D. Sudar, C. Bator-Kelly, M. Bissell, and S. Lelievre. Automated local bright feature image analysis of nuclear protein distribution identifies changes in tissue phenotype. *Proceedings of National Academy of Science*, 103:4445–4450, 2006.
- [3] D. Lowe. *Perceptual Organization and Visual Recognition*. Kluwer Academic Publisher, The Netherlands, 1985.
- [4] R. Malladi, J. Sethian, and B. Vemuri. Shape modeling with front propagation: a level set approach. *IEEE Transactions on Pattern Analysis and Machine Intelligence*, 17:158–175, 1995.
- [5] G. Medioni, M.S. Lee, and C.K. Tang. *A Computational Framework for Segmentation and Grouping*. Elsevier, 2000.
- [6] R. Murphy. Automated interpretation of subcellular locatoin patterns. In *IEEE Int. Symp. on Biomedical Imaging*, pages 53–56, April 2004.
- [7] C. Ortiz De Solorzano, R. Garcia, A. Jones, D. Pinkel, W. Gray, D. Sudar, and S. Lockett. Segmentation of confocal microscope images of cell nuclei in thick tissue section. *Journal of Microscopy*, 193(3):193–212, 1999.
- [8] B. Parvin, Q. Yang, J. Han, H. Chang, B Rydberg, and M. H. Barcellos-Hoff. Iterative voting for inference of structural saliency and characterization of subcellular events. *IEEE Transactions on Image Processing*, March 2007.
- [9] S. Raman, C. A. Maxwell, M. H. Barcellos-Hoff, and B. Parvin. Geometric approach to segmentation and protein localization in cell culture assays. *Journal of Microscopy*, 225:22–30, 2007.
- [10] A. Sarti, C. Ortiz De Solorzano, S. Lockett, and R. Malladi. A geometric model for 3-d confocal image analysis. *IEEE Transactions on Biomedical Engineering*, 47(12):1600–1610, December 2000.
- [11] A. Shashua and S. Ullman. Structural saliency: the detection of globally salient structures using a locally connected network. In *Proceedings of the IEEE International Conference on Computer Vision*, pages 321–327, Tampa, FL, 1988.
- [12] Q. Yang and B. Parvin. Chef: Convex hull of elliptic features for 3d blob detection. In *Proceedings of the International Conference on Pattern Recognition*, Aug 2002.